

## Supplementary Materials and Methods

### Construction of the targeting vector

Construction of the targeting vector, pCAG-C $\Delta$ M20, and the generation of mice carrying the *Xist*<sup>CAG2L</sup> allele were carried out as follows: a 4.6 kb EcoRI-BamHI fragment present in exon1 of the *Xist* gene was cloned into pBluescriptII SK(-), in which SalI and XhoI sites had been destroyed by double digestion and subsequent ligation of the compatible ends. A 4.4-kb EcoRI genomic fragment containing the major transcription start site of *Xist* was subsequently inserted at the EcoRI site of this plasmid in an appropriate orientation to derive p $\Delta$ XS-EB9.0. PCR was carried out on genomic DNA using Mlu-Sal-21F(+)<sub>37</sub> and AS1634F as primers, and a product of about 900 bp was digested with MluI and XhoI and used to replace the endogenous MluI-XhoI fragment present in p $\Delta$ XS-EB9.0 to generate p $\Delta$ M20. In parallel, pCAG-CY NotI (a gift from Hitoshi Niwa), which has a floxed pac-EGFP-pA cassette downstream of the CAG promoter, was digested with NotI to release a 4.0-kb fragment containing the CAG promoter and the floxed cassette. Following the addition of a SalI linker at both ends, this fragment was cloned at the SalI site in p $\Delta$ M20 in an appropriate orientation to generate pCAG-C $\Delta$ M20.

## Preparation of MEFs

$X^{CAG2L}X^{Rb(X.9)}$  and  $X^{CAG2L}X^{JF1}$  fetuses were obtained at E13.5 from  $X^{CAG2L}X$  females crossed with either  $X^{Rb(X.9)}Y$  or JF1 males.  $X^{Rb(X.9)}X^{CAG}$  and  $X^{JF1}X^{CAG}$  fetuses were obtained at E13.5 by crossing [ $X^{CAG2L}Y$ ; *Pgk2-cre*] males with either  $X^{Rb(X.9)}X^{Rb(X.9)}$  or JF1 females. Following a removal of the head and internal organs, the carcass of each fetus placed in a 100-mm dish was minced into vary small pieces through an 18G hypodermic needle attached to a 2.5-ml syringe in 500 ul of PBS and cultured in DMEM/10% FBS for several days and passaged for expansion.

## Primer sequences

Mlu-Sal-21F(+) <sup>37</sup> :	5'-GGC CGT GAC GCG TCG ACA TGT GCC GG TTC TTC CGT GGT-3'
AS1634F	5'-GCG TAA CTG GCT CGA GAA TA-3'
XistEx7F21	5'-GCC CAG GTC ACA TTA TGG TT-3'
XistEx7R20	5'-CTC CAA TTT CTG GGC TCA AG-3'
18SRNA1	5'-TCA AGA ACG AAG TCG GAG GTT-3'
18SRNA2	5'-GCA CAT CTA AGG GCA TCA CAG-3'
Bx-CAG1113F	5'-AAA CTA CAA CCC CCC CTA CAC CCC CCT CCC-3'
Bx-CAG1686R	5'-TTG TTT AGG AGT TGT AGG AAA AAG AAG AAG-3'
Bx-CAG1646R	5'-GTA TGA ATA TGG TTA GTA GAG GTT TTA GAG-3'
XistPr2	5'-AAA TAT TCC CCC AAA ACT CCT TAA ATA A-3'
XistPr3	5'-GTT AAT TAA TGT AGA AGA ATT TTT AGT GTT TA-3'
XistPr4	5'-GGT TTG TTT AAG TAG AAG ATA TAT TGA AAT-3'

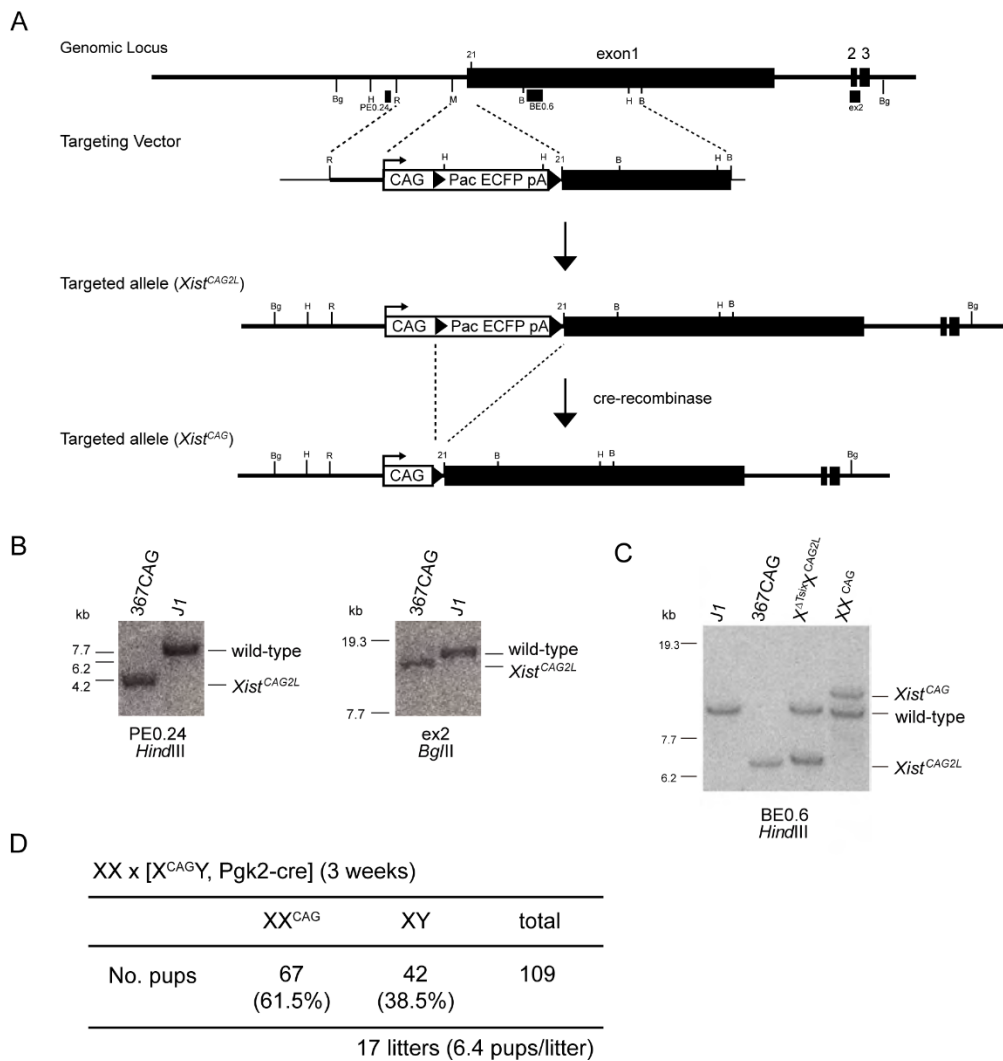


**Fig. S1. Introduction of a constitutively active allele of *Xist* into the mouse**

(A) the targeting scheme for generating the *Xist*<sup>CAG</sup> allele. The endogenous *Xist* promoter was replaced with a CAG-Pac ECFP-pA cassette to produce the *Xist*<sup>CAG2L</sup> allele, which would not produce *Xist* RNA. In the presence of cre recombinase, the *Xist*<sup>CAG2L</sup> allele should be converted into the *Xist*<sup>CAG</sup> allele, which in turn expresses *Xist* constitutively. The locations of the probes (PE0.24, BE0.6, and ex2) used for Southern blotting in B and C are indicated. H, *Hind*III; Bg, *Bgl*II; B, *Bam*HI; R, *Eco*RI; M, *Mlu*I. (B) Homologous recombination was confirmed by Southern blotting. 367CAG is the ES cell line harboring the correct targeting event. Genomic DNA digested with *Hind*III (left) and *Bgl*II (right) was probed with PE0.24 (Sado et al., 2006) and ex2 (a genomic fragment encoding *Xist* exon 2), respectively. (C) The presence of the respective allele was confirmed in mice. Genomic DNA digested with *Hind*III was probed with BE0.6 (Sado et al., 2005). (D) The number of pups recovered from a cross between wild-type females and X<sup>CAG2L</sup>Y males carrying a Pgk2-cre transgene.

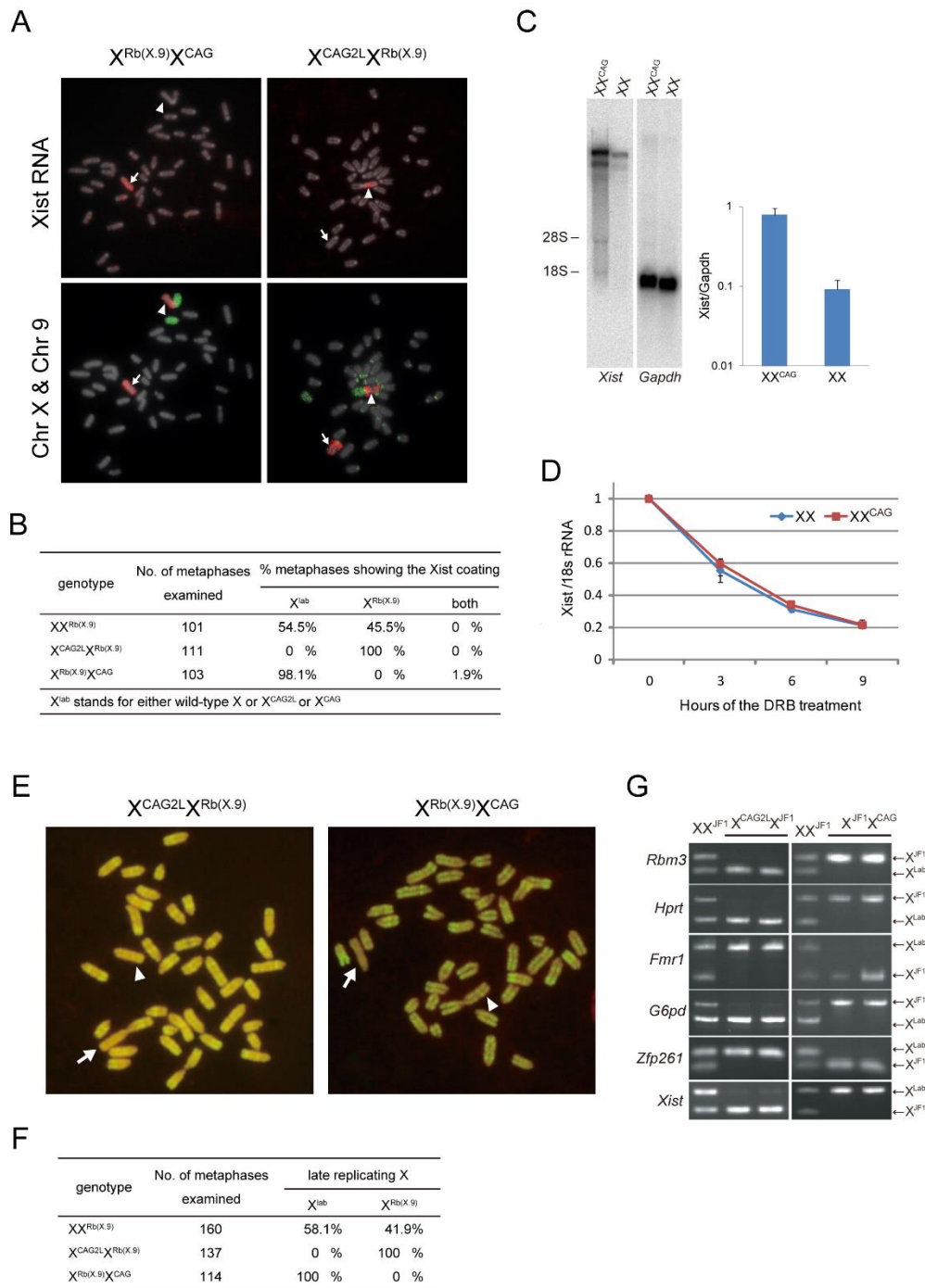


**Fig. S2. The X chromosome carrying the *Xist*<sup>CAG</sup> allele was preferentially inactivated in MEFs.**

(A) Representative images of RNA-FISH and subsequent chromosome painting in MEFs prepared from X<sup>CAG2L</sup>X<sup>Rb(X.9)</sup> and X<sup>Rb(X.9)</sup>X<sup>CAG</sup> fetuses. Upper panels show RNA-FISH detecting *Xist* RNA (red) accumulated on the X chromosome. DNA was counterstained with DAPI (blue). Lower panels show chromosome painting of the same metaphase spread examined by RNA-FISH in the upper

panels using probes specific for the X chromosome (red) and chromosome 9 (green). Arrows indicate morphologically normal wild-type or mutated X, whereas arrowheads indicate  $X^{Rb(X.9)}$ . **(B)** The prevalence of metaphases showing the *Xist* coating with either morphologically normal X (wild-type X,  $X^{CAG2L}$ , and  $X^{CAG}$ ) or  $X^{Rb(X.9)}$ . The accumulation of *Xist* RNA was observed on either X chromosome in  $XX^{Rb(X.9)}$  MEFs, reflecting random X-inactivation. In contrast, *Xist* RNA was found on  $X^{Rb(X.9)}$  in  $X^{CAG2L}X^{Rb(X.9)}$  MEFs, whereas it was essentially confined to the morphologically normal  $X^{CAG}$  in  $X^{Rb(X.9)}X^{CAG}$  MEFs. A minor fraction in  $X^{Rb(X.9)}X^{CAG}$  MEFs (1.9%) showed *Xist* coating on both X chromosomes. This may be due to the transmigration of overexpressed *Xist* RNA from the  $Xist^{CAG}$  allele on  $X^{CAG}$  to the other X as previously reported by Jeon and Lee (Jeon and Lee, 2011). **(C)** The expression of *Xist* in XX and  $XX^{CAG}$  was examined by Northern blotting and quantitative RT-PCR. **(D)** The half-life assay of *Xist* RNA expressed from the  $Xist^{CAG}$  allele.  $XX^{CAG}$  and XX MEFs were treated with DRB, an inhibitor of RNA polymerase II, and RNA was collected at different time points for qRT-PCR. The amount of *Xist* RNA present in MEFs prepared from XX and  $XX^{CAG}$  fetuses at each time point was measured relative to 18s ribosomal RNA by quantitative RT-PCR. **(E)** The replication patterns of chromosomes in  $X^{CAG2L}X^{Rb(X.9)}$  and  $X^{Rb(X.9)}X^{CAG}$  MEFs.  $X^{Rb(X.9)}$  and  $X^{CAG}$  visualized as a pale chromosome in  $X^{CAG2L}X^{Rb(X.9)}$  and  $X^{Rb(X.9)}X^{CAG}$ , respectively (arrows), were referred to as a typical inactive X chromosome. An active counterpart is indicated by arrowheads. 5-Bromo-2-deoxyuridine (BrdU) (100  $\mu$ g/ml) was incorporated into MEFs for 9 hours with Colcemid present at 100 ng/ml in the culture medium during the last hour. Chromosome spreads were stained with Acridine Orange. **(F)** Summary of the replication timing analysis in  $XX^{Rb(X.9)}$ ,  $X^{CAG2L}X^{Rb(X.9)}$ , and  $X^{Rb(X.9)}X^{CAG}$  MEFs, showing the prevalence of respective cells with either  $X^{Lab}$  referring to a morphologically normal X (wild-type X,  $X^{CAG2L}$ , and  $X^{CAG}$ ) or  $X^{Rb(X.9)}$ , which replicated late in the S phase. **(G)** The allelic expression analysis of X-linked genes in MEFs derived from the F1 hybrid fetuses of JF and respective mutant mice. These MEFs allowed us to study the allelic expression of X-linked genes using restriction site polymorphisms between JF1 and laboratory strains. Six X-linked genes (*Rbm3*, *Hprt*, *Fmr1*, *G6pd*, *Zfp261*, and *Xist*) were analyzed by RT-PCR and the subsequent digestion of products with appropriate restriction enzymes. The origin of each fragment is shown on the right:  $X^{Lab}$  refers to either  $X^{CAG2L}$ ,  $X^{CAG}$ , or wild-type X derived;  $X^{JF1}$  refers to the X derived from the JF1 strain.

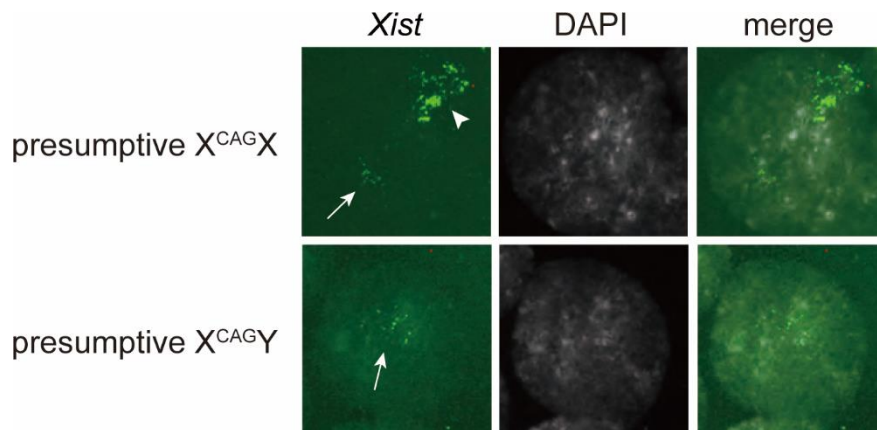


**Fig. S3. RNA-FISH for *Xist* expression in 8-cell embryos recovered from a cross between XX<sup>CAG</sup> females and wild-type males.**

It is likely that the very faint scattered signals (arrows) represented very weak expression of from maternally inherited *Xist*<sup>CAG</sup>. An arrowhead indicates a normal *Xist* cloud.

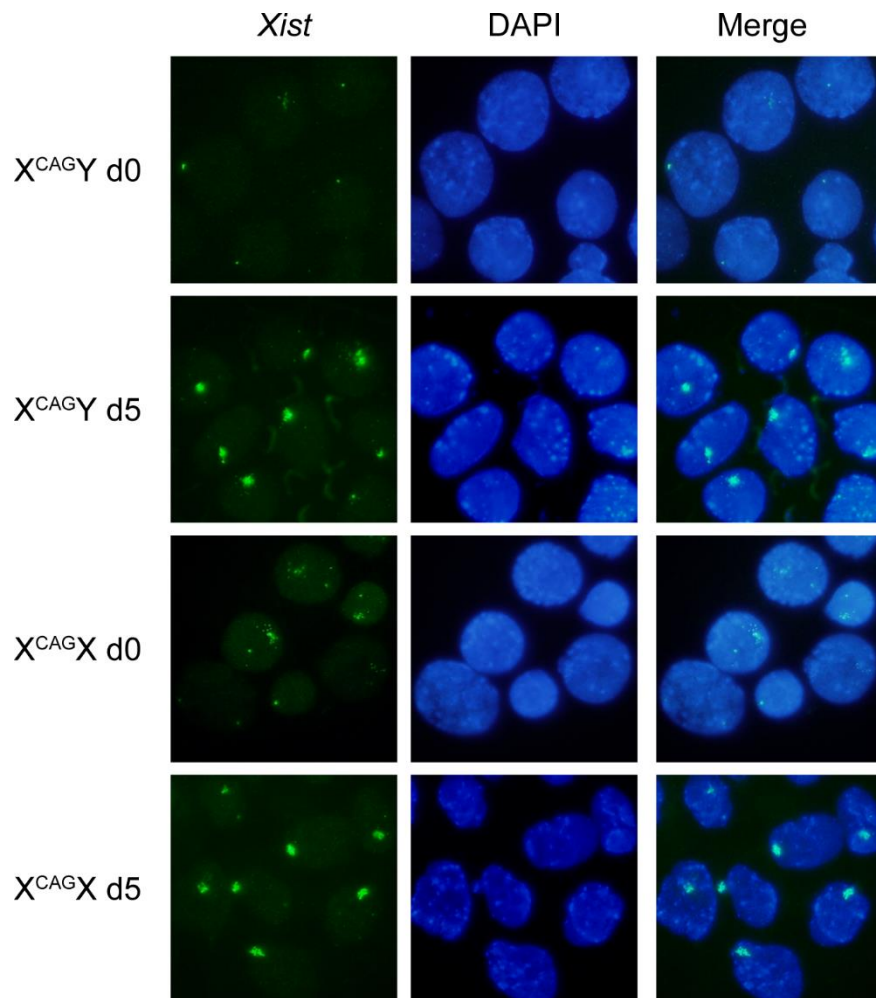


**Fig. S4. RNA-FISH for Xist expression in X<sup>CAGY</sup> and X<sup>CAGX</sup> ES cells before (d0) and after (d5) differentiation.**

The *Xist*<sup>CAG</sup> allele was upregulated in both male and female ES cells upon induction of differentiation. Undifferentiated ES cells were maintained in 2i medium, whereas differentiation was induced into Epiblast-like cells (EpiLCs) according to Hayashi et al (Hayashi et al., 2012).

- Hayashi, K., Ogushi, S., Kurimoto, K., Shimamoto, S., Ohta, H. and Saitou, M.** (2012). Offspring from oocytes derived from in vitro primordial germ cell-like cells in mice. *Science* **338**, 971-975.
- Jeon, Y. and Lee, J. T.** (2011). YY1 tethers Xist RNA to the inactive X nucleation center. *Cell* **146**, 119-133.
- Sado, T., Hoki, Y. and Sasaki, H.** (2005). Tsix silences Xist through modification of chromatin structure. *Developmental cell* **9**, 159-165.
- Sado, T., Hoki, Y. and Sasaki, H.** (2006). Tsix defective in splicing is competent to establish Xist silencing. *Development* **133**, 4925-4931.